



Published in final edited form as:

Cancer Res. 2014 February 1; 74(3): 808–817. doi:10.1158/0008-5472.CAN-13-1655.

Cancer-derived mutations in KEAP1 impair NRF2 degradation but not ubiquitination

Bridgid E. Hast¹, Erica W. Cloer¹, Dennis Goldfarb², Heng Li³, Priscila F. Siesser¹, Feng Yan¹, Vonn Walter⁴, Ning Zheng³, D. Neil Hayes⁵, and Michael B. Major^{1,2}

¹Department of Cell Biology and Physiology, Lineberger Comprehensive Cancer Center, University of North Carolina at Chapel Hill School of Medicine, Box#7295, Chapel Hill, NC 27599, USA

²Department of Computer Science, University of North Carolina at Chapel Hill, Box#3175, Chapel Hill, NC 27599, USA

³Howard Hughes Medical Institute, Department of Pharmacology, University of Washington, Box#357280, Seattle, WA 98195-7280, USA

⁴Lineberger Comprehensive Cancer Center, University of North Carolina at Chapel Hill School of Medicine, Box#7295, Chapel Hill, NC 27599, USA

⁵Department of Internal Medicine and Otolaryngology, Division of Medical Oncology, Lineberger Comprehensive Cancer Center, University of North Carolina at Chapel Hill School of Medicine, Box#7295, Chapel Hill, NC 27599, USA

Abstract

NRF2 is a transcription factor that mediates stress responses. Oncogenic mutations in *NRF2* localize to one of its two binding interfaces with KEAP1, an E3 ubiquitin ligase that promotes proteasome-dependent degradation of NRF2. Somatic mutations in *KEAP1* occur commonly in human cancer, where *KEAP1* may function as a tumor suppressor. These mutations distribute throughout the KEAP1 protein but little is known about their functional impact. In this study, we characterized 18 *KEAP1* mutations defined in a lung squamous cell carcinoma tumor set. Four mutations behaved as wild-type KEAP1, thus are likely passenger events. R554Q, W544C, N469fs, P318fs, and G333C mutations attenuated binding and suppression of NRF2 activity. The remaining mutations exhibited hypomorphic suppression of NRF2, binding both NRF2 and CUL3. Proteomic analysis revealed that the R320Q, R470C, G423V, D422N, G186R, S243C, and V155F mutations augmented the binding of KEAP1 and NRF2. Intriguingly, these 'super-binder' mutants exhibited reduced degradation of NRF2. Cell-based and in vitro biochemical analyses demonstrated that despite its inability to suppress NRF2 activity, the R320Q 'superbinder' mutant maintained the ability to ubiquitinate NRF2. These data strengthen the genetic interactions between KEAP1 and NRF2 in cancer and provide new insight into KEAP1 mechanics.

Introduction

In contrast to the mutational clustering seen in oncogenes, where a few residues are frequently affected, mutations in tumor suppressor proteins typically lack focal enrichment. This creates uncertainty as to the impact of specific mutations on protein function; mutations

Corresponding author: Michael B. Major, Lineberger Comprehensive Cancer Center, University of North Carolina at Chapel Hill Box#7295, Chapel Hill, NC 27599, benmajor@med.unc.edu, Phone: 919-966-9258, Fax: 919-966-8212.

The authors declare no conflicts of interest.

may be phenotypically silent ‘passenger’ events, they may result in a spectrum of hypomorphs, or produce a functionally dead protein. Catalogued associations between specific cancer genotypes and protein function will instruct many principles of cancer biology and oncology, including patient stratification for targeted therapy.

The Cancer Genome Atlas (TCGA) recently reported the characterization of 178 squamous cell lung carcinomas (SQCC), revealing at least 10 recurrently mutated genes. Among these were activating mutations in the *NFE2L2* (*NRF2*) oncogene and presumed loss-of-function mutations within the *KEAP1* tumor suppressor gene, at 15% and 12% of tumors, respectively (1). *KEAP1* functions as a substrate recognition module within the CUL3-based E3 ubiquitin ligase, which targets the *NRF2* transcription factor for proteosomal degradation (2). Regardless of tissue origin, nearly all somatic mutations within *NRF2* fall to either the ETGE or the DLG motif, two regulatory short amino acid sequences within *NRF2* that contact *KEAP1* (3). As such, these mutations liberate *NRF2* from *KEAP1*-mediated ubiquitination. Comparatively, a survey of cancer genomic data revealed 213 somatic mutations dispersed across the full length of the *KEAP1* protein, a pattern consistent with the mutational spread often seen in tumor suppressor genes. Like many discoveries from genomic sequencing efforts, the functional consequences of these *KEAP1* mutations are largely not known.

The lung SQCC analysis revealed that as expected, *KEAP1* mutations and *NRF2* mutations do not co-occur in the same tumor, and that tumors with *KEAP1* or *NRF2* mutations express relatively high levels of *NRF2*-target mRNAs (1, 4). *NRF2* target genes include a host of stress response genes, such as heme oxygenase 1 (*HMOX1*), NADPH dehydrogenase quinone 1 (*NQO1*), and genes involved in glutathione synthesis (5). The expression of these genes strengthens the cellular defense system to neutralize reactive oxygen species (ROS), clear xenobiotic agents, and reprogram protein degradation machinery to restore homeostasis. Recent studies also establish a role for *NRF2* in modulating anabolic pathways to suit the metabolic demands of cancer cell growth, effectively yielding an increase in cancer cell proliferation (6). Although comprehensive data are not complete, several studies have reported that *NRF2* activity correlates with poor prognosis and chemotherapeutic resistance (7–10).

The now established importance of *KEAP1*-*NRF2* in promoting cancer cell growth and survival underscores the need to elucidate how cancer evolution leads to pathway activation. Several mechanisms are easily recognized from cancer genomic studies: activating mutations in *NRF2* free it from *KEAP1* association (11), copy number amplifications of the *NRF2* genomic locus increase protein expression, and *KEAP1* promoter hypermethylation decreases its mRNA and protein expression (12, 13). What remains uncertain is which somatic mutations within *KEAP1* affect its function, to what degree do they impact function, and mechanistically how its function is compromised. Recent efforts from several groups have identified correlations between cancer genotype and phenotype, and these findings may have a significant impact on clinical interventions (14–18). With these concepts in mind, we functionally tested and biochemically characterized *KEAP1* mutations found within lung SQCC. Our data connects cancer-derived *KEAP1* genotypes with *NRF2* phenotype. Unexpectedly, we found that many *KEAP1* mutant proteins bind and ubiquitinate *NRF2*, but do not promote its proteosomal degradation or suppress its transcriptional activity.

Materials and Methods

Tissue culture, transfections, and siRNAs

HEK293T, A549, and H2228 cells were obtained from the American Tissue and Culture Collection, which authenticates cells line using short tandem repeat analysis. Cell lines were

not passaged for more than 6 months after resuscitation. The *Keap1*^{-/-} MEFs were kindly provided by Thomas Kensler and Nobunao Wakabayashi. HEK293T cells were grown in Dulbecco's Modified Eagle's Medium, supplemented with 10% FBS and 1% GlutaMAX (Life Technologies) in a 37°C humidified incubator with 5% CO₂. *Keap1*^{-/-} mouse embryo fibroblasts (MEF) were cultured in IMDM supplemented with 10% FBS. A549 and H2228 cells were grown in RPMI supplemented with 10% FBS. Expression constructs were transfected in HEK293T cells with Lipofectamine 2000 (Life Technologies). A549 cells and *Keap1*^{-/-} MEFs were transfected with Fugene HD (Roche). Transfection of siRNA was done with Lipofectamine RNAiMAX (Life Technologies). siRNA sequences for CUL3 are as follows: (A) 5'-GGU CUC CUG AAU ACC UCU CAU UAU U, (B) 5'-GAA UGU GGA UGU CAG UUC ACG UCA A, (C) 5'-GGA UCG CAA AGU AUA CAC AUA UGU A.

Antibodies and buffers employed for Western blot analysis: anti-FLAG M2 monoclonal (Sigma), anti-HA monoclonal (Roche), anti-βactin polyclonal (Sigma, A2066), anti-βtubulin monoclonal (Sigma, T7816), anti-KEAP1 polyclonal (ProteinTech, Chicago IL), anti-GFP (abcam, ab290), anti-NRF2 H300 polyclonal (Santa Cruz, Santa Cruz CA), anti-SLK (Bethyl, A300-499A), anti-DPP3 (abcam, ab97437), anti-MCM3 (Bethyl, A300-123A), anti-WTX (19), anti-IKKβ (Cell Signaling, 2678), anti-p62/SQSTM (Santa Cruz, sc25575), HMOX1 (abcam, ab13248), anti-CUL3 (Cell Signaling, 2759), anti-MEK1/2 (Cell Signaling, 8727), anti-histone 3 (Cell Signaling, 4499), anti-GST (Cell Signaling, 2622), and anti-VSV polyclonal (Bethyl, A190-131A). 0.1% NP-40 lysis buffer: 10% glycerol, 50mM HEPES, 150 mM NaCl, 2mM EDTA, 0.1% NP-40; RIPA buffer: 0.1% NP-40, 0.1% SDS, 10% glycerol, 25mM Tris HCl, 0.25% sodium deoxycholate, 150mM NaCl, 2mM EDTA.

Immunopurification, cell fractionation, and Western blotting

For FLAG immunopurification, cells were lysed in 0.1% NP-40 lysis buffer. Cell lysates were cleared by centrifugation and incubated with FLAG resin (Sigma) before washing with lysis buffer and eluting with NuPAGE loading buffer (Life Technologies). For immunoprecipitation of endogenous NRF2, cells were lysed in 0.1% NP-40 lysis buffer. Cell lysates were cleared by centrifugation, and pre-cleared for 1 hour with Protein A/G resin (Pierce). Lysates were then incubated with NRF2 H-300 antibody (Santa Cruz) overnight at 4 degree Celsius, and then incubated for 1 hour with Protein A/G resin before eluting with NuPAGE loading buffer. For siRNA, HEK293T cells were transiently transfected and lysed in RIPA buffer 60 hours post transfection. Cell fractionation was performed using the NE-PER Nuclear and Cytoplasmic Extraction Reagent kit (Thermo Scientific).

Plasmids, expression vectors, and site-directed mutagenesis

Expression constructs for the *KEAP1* mutants were generated by PCR-based mutagenesis and sequence verified before use; primer sequences for the mutagenesis are shown in Table S3. The TCGA tumor sample codes for each mutation are also shown in Table S3. The reporter construct for human *hNQO1*-ARE-luciferase was a kind gift from Jeffrey Johnson.

ARE luciferase quantification

Cells were transfected with expression constructs, FLAG-KEAP1, FLAG-NRF2, *hNQO1*-ARE luciferase, and a control plasmid containing *Renilla* luciferase driven by a constitutive cytomegalovirus (CMV) promoter. Approximately 24 hours post-transfection, NRF2-mediated transcription was measured as the ratio of Firefly to *Renilla* luciferase activity (Promega Dual-Luciferase Reporter Assay System).

NRF2 ubiquitination experiments

Ubiquitination of NRF2 under denaturing conditions was performed in HEK293T cells stably expressing FLAG-KEAP1 wild-type or R320Q, VSV-UB1, FLAG-NRF2, and Venus-NPM1. Cells were first lysed in denaturing buffer (25mM Tris, 150mM NaCl, 1% SDS, 1mM EDTA), then diluted with 0.1% NP-40 buffer, followed by immunoprecipitation of NRF2. For *in vitro* ubiquitination studies, GST-tagged wild-type Keap1 and the R320 mutant were over-expressed in Hi5 insect cells and purified using a glutathione affinity column. After removal of the GST tag, the proteins were further purified by ion exchange chromatography. For the *in vitro* ubiquitination assay, wild-type KEAP1 or the R320Q mutant was mixed with recombinant human E1, UbcH5, CUL3-RBX1, ubiquitin and GST-tagged NRF2 NEH2 domain (GST-NRF2-Neh2) in buffer containing 40 mM Tris-HCl pH 8.0, 5 mM MgCl₂, 2 mM DTT and 4 mM ATP. Ubiquitination was carried out at 37 °C and the products were analyzed by Western blot with anti-GST antibody.

Immunostaining

HEK293T cells were cotransfected with the indicated plasmids and plated on 10 µg/mL fibronectin-coated coverslips. Cells were fixed in 4% paraformaldehyde in cytoskeletal buffer for 15 minutes, and coverslips were mounted to slides using the Prolong Gold antifade reagent (Molecular Probes). Images were acquired using a Zeiss LSM5 Pascal Confocal Laser Scanning Microscope equipped with ×63/1.42 Oil PlanApo objective lenses.

Affinity purification and mass spectrometry

For streptavidin and FLAG affinity purification, cells were lysed in 0.1% NP-40 lysis buffer. Cell lysates were incubated with streptavidin or FLAG resin and washed 5 times with lysis buffer. The precipitated proteins were trypsinized directly on beads using the FASP Protein Digestion Kit (Protein Discovery).

Protein identification, filtering, and bioinformatics

All raw data were converted to mzXML format before a search of the resultant spectra using SorcererTM-SEQUEST[®] (build 4.0.4, Sage N Research) and the Transproteomic Pipeline (TPP v4.3.1). Data were searched against the human UniProtKB/Swiss-Prot sequence database (Release 2011_08) supplemented with common contaminants, i.e. porcine (Swiss-Prot P00761) and bovine (P00760) trypsin, and further concatenated with its reversed copy as a decoy (40,494 total sequences). Search parameters used were a precursor mass between 400 and 4500 amu, up to 2 missed cleavages, precursor-ion tolerance of 3 amu, accurate mass binning within PeptideProphet, semi-trypsin digestion, a static carbamidomethyl cysteine modification, variable methionine oxidation, and variable phosphorylation of serines, threonines, and tyrosines. False discovery rates (FDR) were determined by ProteinProphet and minimum protein probability cutoffs resulting in a 1% FDR were selected individually for each experiment. PeptideProphet/ProteinProphet results for each APMS experiment were stored in a local Prohits database. To determine an interacting protein's abundance relative to WT, prey spectral counts were bait normalized by dividing by the bait spectral count, followed by calculating the number of standard deviations from WT (similar to a Z-score), where the standard deviation was computed for each prey individually. Unfiltered data and spectral count normalizations are provided as Supplementary Table S2.

Results

Connecting cancer-derived *KEAP1* mutations with NRF2 activity

A search of the literature and public domain revealed 213 somatic mutations in *KEAP1*, observed across 17 cancer types and multiple cell lines (Table S1). Mapping these mutations onto the KEAP1 primary amino acid sequence revealed a mostly uniform distribution of affected residues (Fig. 1A). The distribution of mutations specifically found in squamous cell lung carcinoma further reiterated the lack of a ‘mutation cluster region’ (Fig. 1A, blue ovals). Of the 18 mutations found in lung SQCC, only two mutations resulted in a truncated protein product (N469fs and P318fs). The remaining 16 missense mutations included the addition of three new cysteine residues (G333C, W544C, and S243C), which might alter KEAP1 reactivity to electrophilic agents. One mutation, V155F occurred in two separate tumors, and interestingly, none of the mutations in KEAP1 were in residues that directly interface with NRF2 (20). Given the importance of KEAP1-NRF2 signaling in cancer and our inability to predict the functional consequences of KEAP1 mutation, we cloned and comparatively evaluated each of the 18 lung SQCC mutations.

To test whether cancer-derived mutations in KEAP1 affect NRF2-driven transcription, we used an engineered reporter system, wherein the luciferase gene is expressed in a NRF2-dependent manner. Ectopic expression of wild-type KEAP1 suppressed NRF2-dependent luciferase expression in HEK293T cells (Fig. 1B). By comparison, the KEAP1 mutants displayed variable suppression of NRF2-driven transcription. Specifically, L231V, S224Y, P318L and R71L suppressed NRF2 as well as wild-type KEAP1; these genotypes represent possible passenger mutations within *KEAP1*. By contrast, N469fs, P318fs, and G333C exhibited a near-null phenotype. Most surprisingly, of the 18 mutants examined, 11 retained partial ability to suppress NRF2-driven transcription. To further validate these data, we tested the panel in the lung adenocarcinoma cell line A549, which express mutant and inactive KEAP1^{G333C}, and in *Keap1* knockout mouse embryo fibroblasts (MEFs). In all three cell lines tested, which vary in *KEAP1* genotype, we observed a consistent pattern of KEAP1-mediated NRF2 suppression (Fig. 1C and D).

At its core, this work sought to isolate and functionally annotate specific *KEAP1* genotypes so that clinical correlations and predictions might be drawn from genome sequence data alone. As such, we tested whether the relative activities of each KEAP1 mutant correlated with the expression of 15 *NRF2* target genes within the lung SQCC TCGA cohort (1, 4). Comparing luciferase activity (Fig. 1B–D) to the NRF2 transcriptional gene signature, we found that mutants that suppress like wild-type KEAP1 associate with decreased NRF2 activity, whereas mutants unable to completely suppress NRF2 correlate with increased NRF2 target gene expression ($p=0.049$; two-sided Wilcoxon Rank Sum Test) (Fig. S1A). Any attempt to further segregate mutations based on luciferase activity did not show a statistically significant correlation in the patient data.

Biochemical characterization of the KEAP1 mutants

Next, we sought molecular insight into how specific mutations differentially impacted KEAP1 function. First, we determined whether the mutants expressed at levels similar to wild-type KEAP1, as non-synonymous mutations often impair protein folding to decrease protein stability. Transient expression from plasmid DNA indicates that the majority of KEAP1 mutants expressed at levels similar to wild-type protein (Fig. 2A and S1B). Further study is required to determine if the reduced expression of mutants R554Q, W544C, N469fs, P318fs, G480W, and G333C is due to altered protein or mRNA stability. To extend these data, the subcellular localization of KEAP1 and each KEAP1 mutant was evaluated in

HEK293T cells; all mutants exhibited a localization pattern indistinguishable from wild-type KEAP1 (Fig. S1C).

KEAP1 functions as a critical sensor of oxidative stress, wherein multiple cysteine residues act as biosensors for ROS and xenobiotic molecules (11, 21, 22). In cells, KEAP1 is thought to exist as a homodimer, creating a 2:1 stoichiometry with the NRF2 substrate. Following cysteine modification, either by reactive oxygen species or electrophilic agents like *tert*-butylhydroquinone (tBHQ), a conformational change within the KEAP1 homodimer creates an SDS-resistant form which is readily visualized under denaturing electrophoresis (23, 24). When treated with the pathway agonist, all 18 mutants formed an SDS-resistant dimer, suggesting that the mutations do not impair dimerization (Fig. 2A). To more rigorously test this, FLAG-tagged KEAP1 mutants were transfected into HEK293T cells stably expressing wild-type hemagglutinin epitope (HA) tagged KEAP1. FLAG immunopurification of the mutant protein, followed by Western blot for the HA-tagged wild-type protein was performed to evaluate KEAP1 dimerization (Fig. 2B). Each KEAP1 mutant protein retained the ability to dimerize with wild-type KEAP1.

The most likely molecular explanation for how KEAP1 mutations compromise its ability to suppress NRF2 is that the mutations impact either the KEAP1-NRF2 association or the KEAP1-CUL3 association. We evaluated whether the KEAP1 mutants maintain their ability to interact with endogenous CUL3 (Fig. S2A). Immunoprecipitation and Western blot analysis revealed that all of the KEAP1 mutants interact with CUL3 (Fig. 2C). Further analysis is needed to determine if the subtle differences in CUL3 binding reflect differential affinities or expression variability (Fig 2C, compare lanes 15, 16, 19). Next we determined if the KEAP1-NRF2 association was maintained among the mutants. Western blot analysis of immunopurified KEAP1 and mutant KEAP1 protein complexes showed that the R554Q, W544C, N469fs, P318fs, and G333C mutants failed to bind NRF2 (Fig. 3A and S2B and S2C). Surprisingly, however, the remaining 13 KEAP1 mutants retained NRF2 binding. Together, these data suggest that with the exception of R554Q, W544C, N469fs, P318fs, and G333C, SQCC-derived KEAP1 mutants maintain their ability to bind both NRF2 and CUL3.

Mass spectrometry-based proteomic analysis of KEAP1 revealed 42 high confidence associated proteins (4). To gather a global perspective of how the mutations affect KEAP1 protein interactions, we performed two experiments. First, we tested the association of 7 high confidence interacting proteins by immunoprecipitation and Western blot analysis. The data show a distinct pattern among the KEAP1 mutants; those that do not bind NRF2 fail to bind several of the known interactors, including SLK, AMER1 (WTX), MCM3, DPP3, and IKBKB (IKK β) (Fig. 3A and S2C). Interestingly, all of these proteins contain an ETGE motif (4). Two mutations, G480W and S224Y, show decreased binding to SLK, MCM3, and DPP3 as compared to NRF2 (Fig. 3A, lanes 8, 15). Second, we employed affinity purification and shotgun mass spectrometry to define and compare the protein interaction network for wild-type KEAP1 and the following mutants: R554Q, R320Q, R470C, G480W, G423V, D422N, G186R, S243C, and V155F (Fig. 3B and Table S2). The unbiased proteomic screens confirm the Western blot results and further expand the pattern of altered protein interactions.

A class of KEAP1 mutants with increased NRF2 binding

We were particularly intrigued with a subset of mutants that consistently bound more NRF2 than wild-type KEAP1 (Fig. 3A, lanes 3, 5, 6, 9, 14, 16, 19, and Fig. S2C). We collectively refer to these mutants as the 'superbinders', although relative protein affinity is not meant to be inferred. The superbinder mutants include R320Q, R470C, G423V, D422N, G186R, S243C and V155F. Increased abundance of NRF2 within each superbinder protein complex

was confirmed by immunoprecipitation and quantitative Western blot analysis (Fig. S3A and S3B). Additionally, label-free mass spectrometry comparing wild-type KEAP1 and two superbinder mutants (R320Q and R470C) showed an increased abundance of NRF2 as compared to wild-type KEAP1; based on spectral counts, R320Q and R470C bound 3.3 and 3.2 fold more NRF2 than wild-type KEAP1, respectively (Fig. 3B and Table S2). For comparative purposes, we performed quantitative proteomic analysis on two non-superbinder mutant proteins: R554Q, which cannot bind NRF2 and G480W, which binds NRF2 similarly to wild-type (Fig. 3B).

Despite an increased level of associated NRF2, the superbinder mutants were unable to suppress NRF2-mediated transcription of an artificial reporter gene (Fig. 1B–D). To confirm this using endogenous metrics of NRF2 activity, HEK293T cells, H2228 cells or A549 cells were transiently transfected with wild-type KEAP1 or the superbinder mutants before Western blot analysis of NRF2 and the NRF2 target gene HMOX1. Transient expression of each superbinder strongly increased the levels of NRF2 and HMOX1 in the H2228 and A549 cell lines (Fig. 4A and B). Subcellular fractionation of the HEK293T cells further revealed that KEAP1 superbinder expression increased the levels of NRF2 within the nuclear compartment (Fig. 4C and S3C).

KEAP1 ‘superbinder’ mutants facilitate NRF2 ubiquitination but not degradation

Our functional and biochemical examination revealed 7 KEAP1 mutations that show significantly impaired ability to suppress NRF2, but yet unexpectedly bind more NRF2 than wild-type KEAP1. To gain further insight, we evaluated NRF2 protein turnover and ubiquitination following KEAP1 superbinder expression. Using a cycloheximide pulse-chase approach, NRF2 protein half-life was evaluated in HEK293T cells stably expressing: 1) wild-type KEAP1, 2) the R320Q superbinder, 3) R470C superbinder, 3) R554Q which does not bind NRF2, or 5) G480W which behaves like wild-type. The expression of R320Q or R470C dramatically stabilized the NRF2 protein as compared to no exogenous KEAP1, wild-type KEAP1 or G480W (Fig. S3D and Fig. 5A). The increased NRF2 stability occurred as a result of binding R320Q or R470C, as unbound NRF2 in the flow-through eluate showed elevated levels but dynamic turnover (Fig. 5B, compare flow-through to KEAP1 immunopurification). Together, these data suggest that the superbinder mutations within KEAP1 result in the stabilization of KEAP1-associated NRF2 and elevated levels of free NRF2, although the free NRF2 is still subject to dynamic turnover.

Given the increased NRF2 association and protein stability, we hypothesized that R320Q and other superbinder mutants impair NRF2 ubiquitination. To test this, we performed two complementary experiments to evaluate NRF2 ubiquitination by wild-type KEAP1 or the R320Q superbinder. First, Western blot analysis of immunoprecipitated NRF2, after denaturation, showed robust ubiquitination by both wild-type KEAP1 and R320Q (Fig. 5C). Second, we performed *in vitro* ubiquitination reactions using purified proteins (Fig. 5D). Remarkably, both experimental approaches demonstrate that wild-type KEAP1 and R320Q ubiquitinate NRF2.

Discussion

With some latitude, we can classify the 18 *KEAP1* mutations into three classes. First, the L231V, S224Y, P318L and R71L mutations did not impact the KEAP1-NRF2 association or the suppression of NRF2 activity. These mutations likely represent passenger events within KEAP1, at least with respect to NRF2. Second, and not surprisingly, the frame shift mutations N469fs and P318fs, as well as G333C, R554Q and W544C did not bind NRF2 and did not or weakly suppressed NRF2-mediated transcription. These genotypes represent null or near-null alleles. Third, the remaining nine mutations fell within a hypomorphic

phenotypic range, with suppression occurring between 30–60% of the wild-type KEAP1. Biochemically, the hypomorphic mutants displayed either reduced NRF2 binding or surprisingly, increased binding (the superbinders).

Mutations in tumor suppressor genes often results in complete loss of protein expression or the expression of a truncated protein product (25). It is therefore intriguing to consider why *KEAP1* is rarely lost through genomic deletion, despite being located between the *SMARCA4* and *STK11* tumor suppressor genes on 19p (cBioPortal). A number of loosely connected observations raise the possibility that KEAP1 may exert cancer-relevant functions that extend beyond regulation of oxidative stress and NRF2. First, we found that many KEAP1 mutations result in a hypomorphic phenotype, rather than a genetic null. Second, in general, these hypomorphic mutations do not affect the global KEAP1 protein interaction network, suggesting that some KEAP1 protein interactions are retained in the absence of NRF2 suppression (Fig. 3B and Table S2). Indeed, KEAP1 associated proteins regulate a number of disparate cellular processes, including cell cycle, migration, and apoptosis (4, 26–34). Third, while the presence and importance of NRF2-independent KEAP1 functions remain unknown, we and others have established that several KEAP1 interacting proteins drive NRF2 activation via a competitive binding mechanism (4, 19, 35–37). Previously, we found that hypomorphic *KEAP1* mutants can be further inactivated by the ETGE-containing competitive binding protein, DPP3(4). Coupled with the observed over-expression of *DPP3* in lung squamous cell carcinoma, these observations suggest that from the perspective of cancer cell fitness, the presence of a hypomorphic *KEAP1* mutation may be more valuable than a null mutant.

The most surprising and perhaps exciting discovery we observed was the identification of the ‘superbinders’—those that do not suppress NRF2-mediated transcription, exhibit enhanced binding to NRF2, and facilitate NRF2 ubiquitination. Three points of discussion are appropriate. First, by what mechanism could the ‘superbinder’ mutations affect NRF2 stability? Several possibilities exist, including an increased affinity between KEAP1 and NRF2 as a means to suppress substrate turn-over. Analogously, the expression of a superbinder variant SH2 domain antagonizes epidermal growth factor signaling via competitive inhibition (38). That said, although studies are ongoing, the lack of a focal enrichment within the tertiary structure casts some doubt on this possibility (Fig. 5E). Cullin ring E3 ubiquitin ligases cycle through an active and inactive state, and this neddylation-dependent transitioning is required for substrate turnover. A second possibility is that the superbinder mutations simply slow the rate of CUL3 neddylation. Finally, proteasome-mediated substrate degradation requires several steps, including recognition, unfolding, translocation, and deubiquitination prior to proteolysis (39). The striking observation that the enhanced NRF2 binding class of *KEAP1* mutants ubiquitinates NRF2 suggests that the mutations functionally hinder one of the steps prior to proteolysis, but after ubiquitination. Here, immediate questions include whether the superbinder mutations affect the ubiquitin chain linkage on NRF2 or whether they perturb the interaction of KEAP1 with the proteasome. All three of these putative mechanisms to describe the superbinder phenotype would inactivate KEAP1 and stabilize NRF2 in a manner consistent with the widely accepted “saturation model” (22). Importantly, as the *KEAP1* mutants described in this study exhibit hypomorphic phenotypes, the superbinders could represent a novel mechanism cancer cells employ to enhance cellular fitness without compromising all cellular functions of multifunctional proteins.

Second, it is now widely accepted that elevated levels of NRF2 are associated with enhanced cell viability in several tumor types (7, 10, 40–42). Although we show that ‘superbinder’ mutations result in NRF2 transcriptional activation, further studies are required to determine whether this KEAP1 mutant class is capable of enhancing cancer cell fitness *in vivo*, and

whether that depends upon prolonged activation of NRF2. Additionally, given emerging evidence identifying other putative KEAP1 substrates in cancer-relevant pathways, such as IKK β within NF- κ B signaling (5, 43), investigating how—if at all—superbinder mutations impact these proteins could also have clinical significance. Looking at the full set of *KEAP1* mutant tumors and the expression of 15 NRF2 target genes, a marginal but statistically significant difference was observed between phenotypically ‘silent’ KEAP1 mutations and mutations which suppress KEAP1-driven NRF2 degradation (Fig. S1A). Our attempts to more precisely correlate *KEAP1* genotype with the cell-based phenotypic scoring failed to reach statistical significance. This is not surprising given the multitude of signaling and metabolic inputs that control KEAP1.

Third, from a structural perspective, we noted weak correlation between the tertiary position of a mutation and whether the mutation produced a KEAP1 superbinder (Fig. 5E). Although speculative, the superbinder mutations appear to be localized at positions that might orient the relative position of IVR and KELCH domains; experiments testing this model are ongoing. Intriguingly, of the 181 missense mutations reported in KEAP1, 6 directly target the R320 superbinder residue, making it the most commonly affected amino acid in KEAP1 (Fig. 1A). Beyond the superbinder mutations, mapping all SQCC 19 mutations onto the KEAP1 structure failed to reveal a discernible pattern. Likewise, side-chain biochemistry for the mutations varies widely, including those within the superbinder class. Cysteine reactivity depends upon the local chemical microenvironment, which is largely dictated by the surrounding amino acids in a protein tertiary structure. Hence, for a cysteine-dependent biosensor like KEAP1, oncogenesis may partially suppress KEAP1 activity by selecting for mutations which add cysteines (S243C, G333C, R470C) or which reduce the relative pKa of existing cysteines, making them more sensitive to electrophilic attack (44). Clearly, spatial constraints preclude the random addition of cysteines as a means to increase the reactivity of KEAP1 to oxidative stress. New cancer-derived cysteines of functional importance would occupy specific localizations within the folded protein. By extension of this idea, cancer-derived mutations that create ‘hyperactive’ cysteines within KEAP1 would be expected to produce a hypomorphic phenotype, as we have observed. Further study is needed to support these ideas, perhaps through the functional and biochemical characterization of the other 213 cancer-derived mutations in *KEAP1*. To this end, medium-throughput functional analysis is facilitated by Gateway-based cloning, outsourced mutagenesis and a strong pathway-specific transcriptional reporter. The resulting data may better enable predictions of genotype-phenotype relationships. However, based on the KEAP1 data presented here, it is not yet possible to derive functional conclusions from the location of a mutation or the type of residue substitution.

In summary, we describe the functional and biochemical characteristics of 18 mutations in the E3 ligase adaptor protein KEAP1, which were found in patient-derived lung cancers. We show that while most of these mutations maintain similar protein interactions to wild-type KEAP1, all but four exhibit hypomorphic or null activity with respect to suppression of NRF2-mediated transcription. Intriguingly, a subset of these mutations exhibit enhanced binding to NRF2 despite an inability to suppress NRF2 activity. Functional analysis of one of these mutants, R320Q, revealed that these mutants are still able to ubiquitinate NRF2, but appear to be unable to facilitate its degradation. Further studies are required to elucidate the mechanism of this class of *KEAP1* mutations, including how they interact with the proteasome, as well as whether these mutants enhance viability of cancer cells via prolonged activation of NRF2.

Supplementary Material

Refer to Web version on PubMed Central for supplementary material.

Acknowledgments

We thank members of the Major lab for critical review of the manuscript. M.B.M. is supported by the NIH through the NIH Director's New Innovator Award, 1-DP2-OD007149-01 and a Scholar Award from the Sidney Kimmel Cancer Foundation. D.N.H is supported by grants from The Cancer Genome Atlas (NIH U24 CA143848 and NIH U24 CA143848-02S1). D.N.H and M.B.M are additionally supported by a grant from the Greensboro Golfers Against Cancer. E.C is supported by the Cancer Cell Biology Training Program, T32-CA09475. N.Z is funded by the HHMI.

References

1. Comprehensive genomic characterization of squamous cell lung cancers. *Nature*. 2012; 489:519–525. [PubMed: 22960745]
2. Furukawa M, Xiong Y. BTB protein Keap1 targets antioxidant transcription factor Nrf2 for ubiquitination by the Cullin 3-Roc1 ligase. *Mol Cell Biol*. 2005; 25:162–171. [PubMed: 15601839]
3. Tong KI, Katoh Y, Kusunoki H, Itoh K, Tanaka T, Yamamoto M. Keap1 recruits Neh2 through binding to ETGE and DLG motifs: characterization of the two-site molecular recognition model. *Mol Cell Biol*. 2006; 26:2887–2900. [PubMed: 16581765]
4. Hast BE, Goldfarb D, Mulvaney KM, Hast MA, Siesser PF, Yan F, et al. Proteomic analysis of ubiquitin ligase KEAP1 reveals associated proteins that inhibit NRF2 ubiquitination. *Cancer Res*. 2013; 73:2199–2210. [PubMed: 23382044]
5. Wakabayashi N, Slocum SL, Skoko JJ, Shin S, Kensler TW. When NRF2 talks, who's listening? *Antioxid Redox Signal*. 2010; 13:1649–1663. [PubMed: 20367496]
6. Mitsuishi Y, Taguchi K, Kawatani Y, Shibata T, Nukiwa T, Aburatani H, et al. Nrf2 redirects glucose and glutamine into anabolic pathways in metabolic reprogramming. *Cancer Cell*. 2012; 22:66–79. [PubMed: 22789539]
7. Jiang T, Chen N, Zhao F, Wang XJ, Kong B, Zheng W, et al. High levels of Nrf2 determine chemoresistance in type II endometrial cancer. *Cancer Res*. 2010; 70:5486–5496. [PubMed: 20530669]
8. Mahaffey CM, Zhang H, Rinna A, Holland W, Mack PC, Forman HJ. Multidrug-resistant protein-3 gene regulation by the transcription factor Nrf2 in human bronchial epithelial and non-small-cell lung carcinoma. *Free Radic Biol Med*. 2009; 46:1650–1657. [PubMed: 19345732]
9. Rushworth SA, Zaitseva L, Murray MY, Shah NM, Bowles KM, MacEwan DJ. The high Nrf2 expression in human acute myeloid leukemia is driven by NF-kappaB and underlies its chemoresistance. *Blood*. 2012; 120:5188–5198. [PubMed: 23077289]
10. Abazeed ME, Adams DJ, Hurov KE, Tamayo P, Creighton CJ, Sonkin D, et al. Integrative radiogenomic profiling of squamous cell lung cancer. *Cancer Res*. 2013
11. Hayes JD, McMahon M. NRF2 and KEAP1 mutations: permanent activation of an adaptive response in cancer. *Trends Biochem Sci*. 2009; 34:176–188. [PubMed: 19321346]
12. Muscarella LA, Parrella P, D'Alessandro V, la Torre A, Barbano R, Fontana A, et al. Frequent epigenetics inactivation of KEAP1 gene in non-small cell lung cancer. *Epigenetics : official journal of the DNA Methylation Society*. 2011; 6:710–719. [PubMed: 21610322]
13. Hanada N, Takahata T, Zhou Q, Ye X, Sun R, Itoh J, et al. Methylation of the KEAP1 gene promoter region in human colorectal cancer. *BMC Cancer*. 2012; 12:66. [PubMed: 22325485]
14. Jaiswal BS, Kljavin NM, Stawiski EW, Chan E, Parikh C, Durinck S, et al. Oncogenic ERBB3 Mutations in Human Cancers. *Cancer Cell*. 2013; 23:603–617. [PubMed: 23680147]
15. Safaee M, Clark AJ, Oh MC, Ivan ME, Bloch O, Kaur G, et al. Overexpression of CD97 Confers an Invasive Phenotype in Glioblastoma Cells and Is Associated with Decreased Survival of Glioblastoma Patients. *PLoS One*. 2013; 8:e62765. [PubMed: 23658650]
16. Hakimi AA, Ostrovnaya I, Reva BA, Schultz N, Chen YB, Gonen M, et al. Adverse Outcomes in Clear Cell Renal Cell Carcinoma with Mutations of 3p21 Epigenetic Regulators BAP1 and SETD2: a Report by MSKCC and the KIRC TCGA Research Network. *Clin Cancer Res*. 2013
17. Meng X, Cai C, Wu J, Cai S, Ye C, Chen H, et al. TRPM7 mediates breast cancer cell migration and invasion through the MAPK pathway. *Cancer Lett*. 2013; 333:96–102. [PubMed: 23353055]

18. Wu YM, Su F, Kalyana-Sundaram S, Khazanov N, Ateeq B, Cao X, et al. Identification of Targetable FGFR Gene Fusions in Diverse Cancers. *Cancer discovery*. 2013
19. Camp ND, James RG, Dawson DW, Yan F, Davison JM, Houck SA, et al. Wilms tumor gene on the X chromosome (WTX) inhibits the degradation of NRF2 through competitive binding to KEAP1. *J Biol Chem*. 2012
20. Lo SC, Li X, Henzl MT, Beamer LJ, Hannink M. Structure of the Keap1:Nrf2 interface provides mechanistic insight into Nrf2 signaling. *The EMBO journal*. 2006; 25:3605–3617. [PubMed: 16888629]
21. Cullinan SB, Gordan JD, Jin J, Harper JW, Diehl JA. The Keap1-BTB protein is an adaptor that bridges Nrf2 to a Cul3-based E3 ligase: oxidative stress sensing by a Cul3-Keap1 ligase. *Mol Cell Biol*. 2004; 24:8477–8486. [PubMed: 15367669]
22. Zhang DD, Lo SC, Cross JV, Templeton DJ, Hannink M. Keap1 is a redox-regulated substrate adaptor protein for a Cul3-dependent ubiquitin ligase complex. *Mol Cell Biol*. 2004; 24:10941–10953. [PubMed: 15572695]
23. Rachakonda G, Xiong Y, Sekhar KR, Stamer SL, Liebler DC, Freeman ML. Covalent modification at Cys151 dissociates the electrophile sensor Keap1 from the ubiquitin ligase CUL3. *Chem Res Toxicol*. 2008; 21:705–710. [PubMed: 18251510]
24. Fourquet S, Guerois R, Biard D, Toledano MB. Activation of NRF2 by nitrosative agents and H₂O₂ involves KEAP1 disulfide formation. *J Biol Chem*. 2010; 285:8463–8471. [PubMed: 20061377]
25. Levine AJ. The tumor suppressor genes. *Annu Rev Biochem*. 1993; 62:623–651. [PubMed: 8394683]
26. Fujibuchi T, Abe Y, Takeuchi T, Imai Y, Kamei Y, Murase R, et al. AIP1/WDR1 supports mitotic cell rounding. *Biochem Biophys Res Commun*. 2005; 327:268–275. [PubMed: 15629458]
27. Kato A, Kurita S, Hayashi A, Kaji N, Ohashi K, Mizuno K. Critical roles of actin-interacting protein 1 in cytokinesis and chemotactic migration of mammalian cells. *Biochem J*. 2008; 414:261–270. [PubMed: 18494608]
28. Takei Y, Tsujimoto G. Identification of a novel MCM3-associated protein that facilitates MCM3 nuclear localization. *J Biol Chem*. 1998; 273:22177–22180. [PubMed: 9712829]
29. Kubota Y, Mimura S, Nishimoto S, Takisawa H, Nojima H. Identification of the yeast MCM3-related protein as a component of Xenopus DNA replication licensing factor. *Cell*. 1995; 81:601–609. [PubMed: 7758114]
30. Young MR, Tye BK. Mcm2 and Mcm3 are constitutive nuclear proteins that exhibit distinct isoforms and bind chromatin during specific cell cycle stages of *Saccharomyces cerevisiae*. *Mol Biol Cell*. 1997; 8:1587–1601. [PubMed: 9285827]
31. Wagner S, Flood TA, O'Reilly P, Hume K, Sabourin LA. Association of the Ste20-like kinase (SLK) with the microtubule. Role in Rac1-mediated regulation of actin dynamics during cell adhesion and spreading. *J Biol Chem*. 2002; 277:37685–37692. [PubMed: 12151406]
32. Wagner S, Storbeck CJ, Roovers K, Chaar ZY, Kolodziej P, McKay M, et al. FAK/src-family dependent activation of the Ste20-like kinase SLK is required for microtubule-dependent focal adhesion turnover and cell migration. *PLoS One*. 2008; 3:e1868. [PubMed: 18382658]
33. Sabourin LA, Rudnicki MA. Induction of apoptosis by SLK, a Ste20-related kinase. *Oncogene*. 1999; 18:7566–7575. [PubMed: 10602516]
34. Hao W, Takano T, Guillemette J, Papillon J, Ren G, Cybulsky AV. Induction of apoptosis by the Ste20-like kinase SLK, a germinal center kinase that activates apoptosis signal-regulating kinase and p38. *J Biol Chem*. 2006; 281:3075–3084. [PubMed: 16316999]
35. Ma J, Cai H, Wu T, Sobhian B, Huo Y, Alcivar A, et al. PALB2 interacts with KEAP1 to promote NRF2 nuclear accumulation and function. *Mol Cell Biol*. 2012; 32:1506–1517. [PubMed: 22331464]
36. Komatsu M, Kurokawa H, Waguri S, Taguchi K, Kobayashi A, Ichimura Y, et al. The selective autophagy substrate p62 activates the stress responsive transcription factor Nrf2 through inactivation of Keap1. *Nature cell biology*. 2010; 12:213–223.

37. Chen W, Sun Z, Wang XJ, Jiang T, Huang Z, Fang D, et al. Direct interaction between Nrf2 and p21(Cip1/WAF1) upregulates the Nrf2-mediated antioxidant response. *Mol Cell*. 2009; 34:663–673. [PubMed: 19560419]
38. Kaneko T, Huang H, Cao X, Li X, Li C, Voss C, et al. Superbinder SH2 domains act as antagonists of cell signaling. *Sci Signal*. 2012; 5:ra68. [PubMed: 23012655]
39. Finley D. Recognition and processing of ubiquitin-protein conjugates by the proteasome. *Annu Rev Biochem*. 2009; 78:477–513. [PubMed: 19489727]
40. Ohta T, Iijima K, Miyamoto M, Nakahara I, Tanaka H, Ohtsuji M, et al. Loss of Keap1 function activates Nrf2 and provides advantages for lung cancer cell growth. *Cancer Res*. 2008; 68:1303–1309. [PubMed: 18316592]
41. Konstantinopoulos PA, Spentzos D, Fountzilias E, Francoeur N, Sanisetty S, Grammatikos AP, et al. Keap1 mutations and Nrf2 pathway activation in epithelial ovarian cancer. *Cancer Res*. 2011; 71:5081–5089. [PubMed: 21676886]
42. Cong ZX, Wang HD, Wang JW, Zhou Y, Pan H, Zhang DD, et al. ERK and PI3K signaling cascades induce Nrf2 activation and regulate cell viability partly through Nrf2 in human glioblastoma cells. *Oncol Rep*. 2013
43. Kim JE, You DJ, Lee C, Ahn C, Seong JY, Hwang JI. Suppression of NF-kappaB signaling by KEAP1 regulation of IKKbeta activity through autophagic degradation and inhibition of phosphorylation. *Cell Signal*. 2010; 22:1645–1654. [PubMed: 20600852]
44. McMahon M, Lamont DJ, Beattie KA, Hayes JD. Keap1 perceives stress via three sensors for the endogenous signaling molecules nitric oxide, zinc, and alkenals. *Proc Natl Acad Sci U S A*. 2010; 107:18838–18843. [PubMed: 20956331]

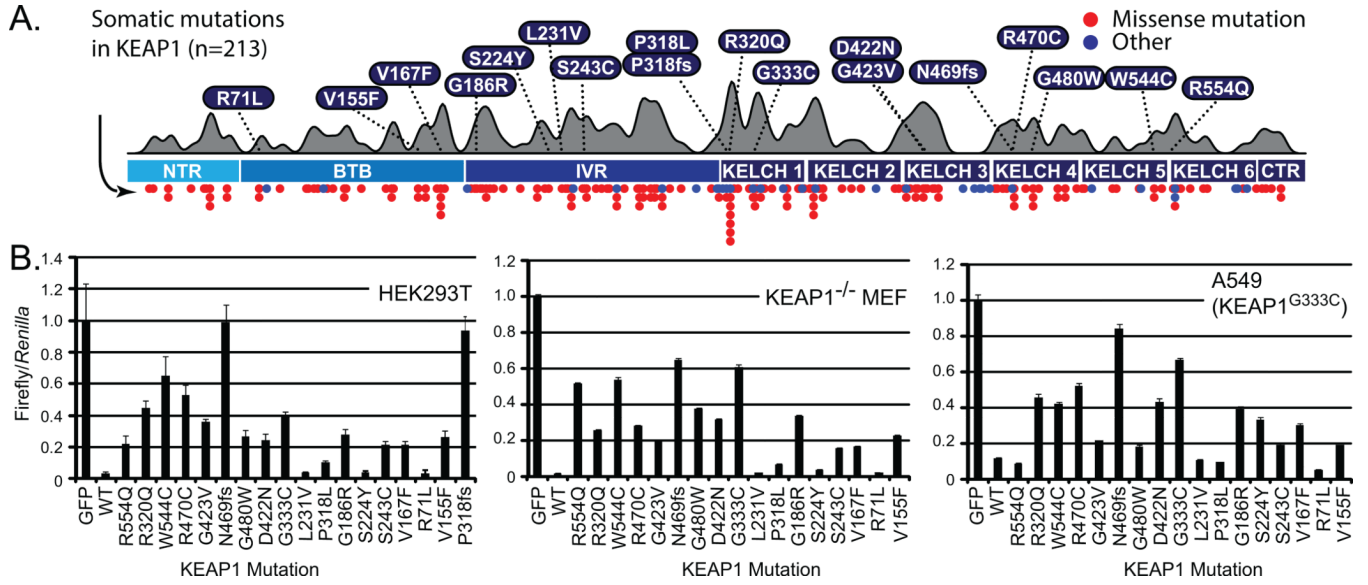


Figure 1. Mutations in *KEAP1* positively correlate with increased NRF2 activity

A, Probability density function of *KEAP1* mutations were approximated using kernel density estimation. Lung SQCC mutations examined in this study are annotated above; all mutations from the public domain are shown below and in Table S1. B–D, HEK293T cells (B), *Keap1* knockout mouse embryo fibroblasts (C), and A549 cells (D) were transiently transfected with the indicated plasmids along with constitutively expressed *Renilla* luciferase, and the *NQO1* promoter driving Firefly luciferase. Cells were lysed and Firefly luciferase values were normalized to the luciferase activity of the *Renilla* control. Error bars represent SD from the mean over three biological replicates (NTR, N-terminal region; BTB, tramtrack and bric-a-brac; IVR, intervening region; CTR, C-terminal region).

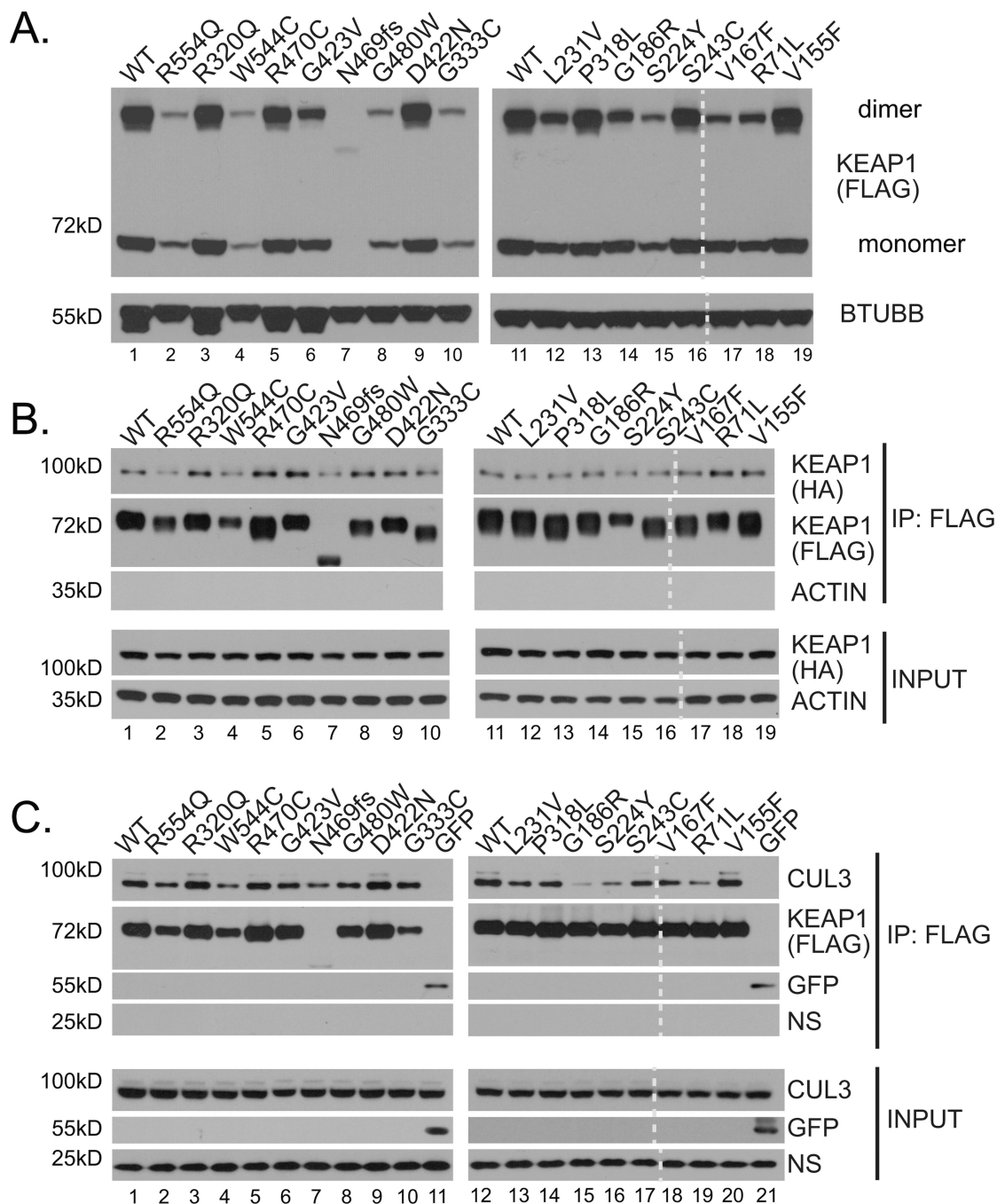


Figure 2. SQCC *KEAP1* mutants retain the ability to dimerize and interact with the CUL3 E3 ubiquitin ligase

A, HEK293T cells were transiently transfected with the indicated *KEAP1* mutant plasmids, and treated with 50 μ M tert-butylhydroquinone (tBHQ) for one hour. Cells were lysed in RIPA buffer and expression of FLAG tagged mutants was analyzed by Western blot for the indicated proteins. The vertical dotted line depicts the digital removal of a *KEAP1* mutant recently found not to exist. The correct mutation, P318fs, is shown in Fig.S2. B, HEK293T cells stably expressing WT HA-*KEAP1* were transiently transfected with the indicated FLAG-tagged *KEAP1* mutants. Cells were lysed in 0.1% NP-40 buffer and immunoprecipitation (IP) of the FLAG-tagged protein complexes were analyzed by Western

blot for the indicated proteins (HA, Hemagglutinin). C, FLAG-tagged protein complexes were immunopurified from HEK293T cells transiently expressing the indicated *KEAP1* mutants and analyzed by Western blot for the indicated proteins (NS, non-specific).

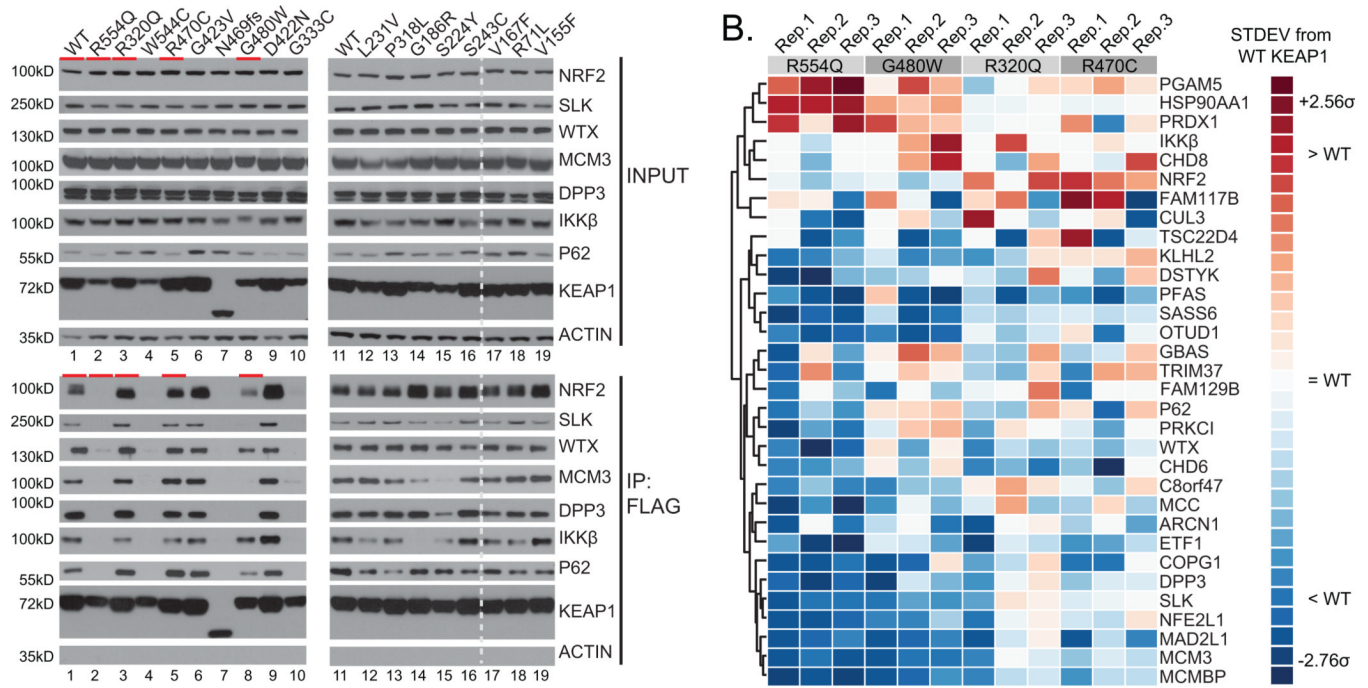


Figure 3. KEAP1 mutant proteins exhibit differential binding to interacting proteins

A. HEK293T cells expressing the indicated KEAP1 mutants were treated with 10 μ M MG132 for one hour, followed by FLAG immunopurification. Protein complexes of the FLAG-tagged mutants were analyzed by Western blot for the indicated proteins. Red lines indicate KEAP1 mutants that were analyzed by mass spectrometry as indicated in (B). **B.** Affinity purification and mass spectrometry (APMS) experiments were performed via affinity purification of streptavidin-tagged KEAP1 mutants from stable HEK293T cells followed by MS analysis of the bound proteins. Colors represent normalized spectral counts – semi-quantitative values that reflect protein abundance – from the APMS experiments. Proteins displayed are previously identified high-confidence KEAP1 interactors.

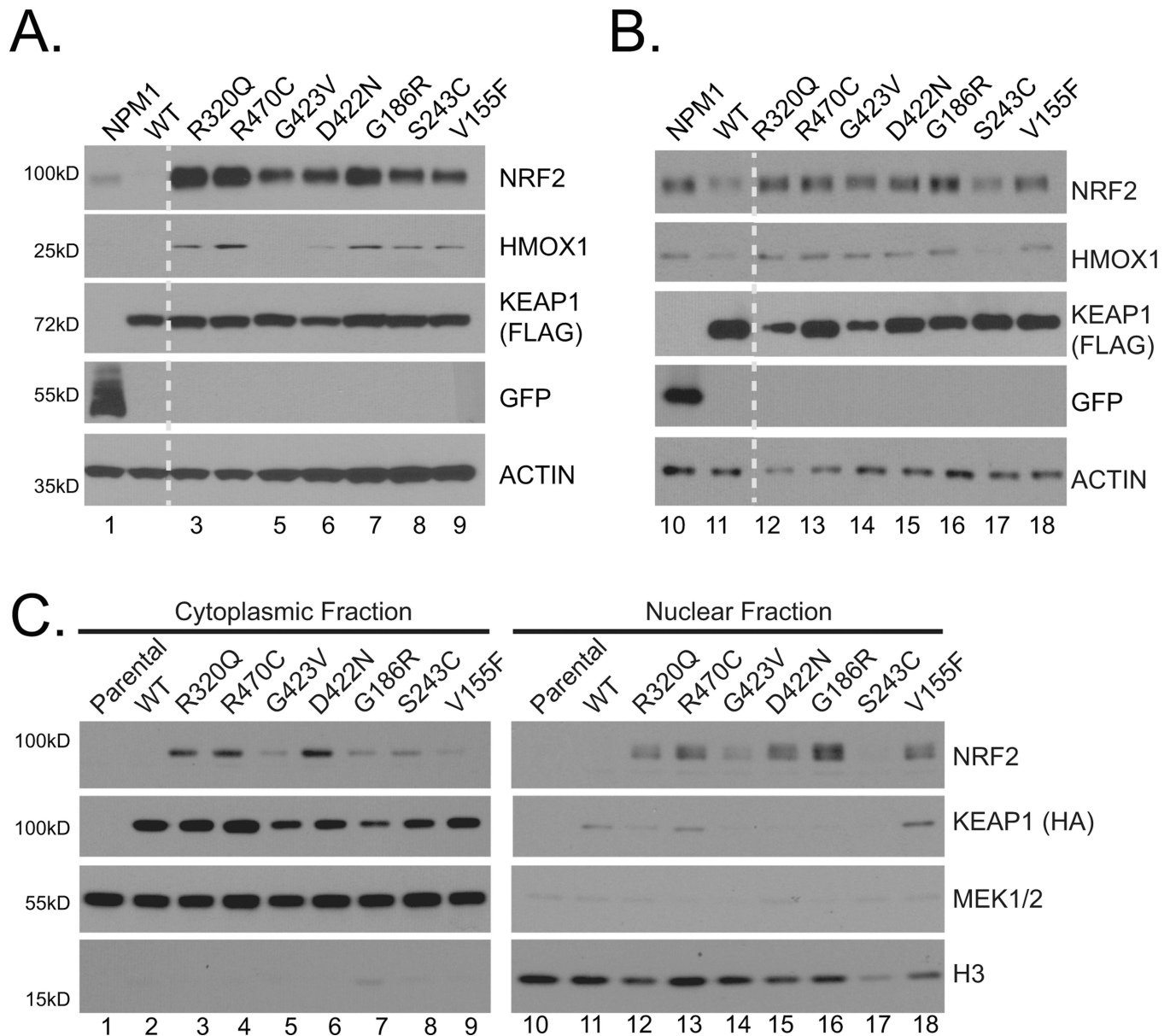


Figure 4. Expression of KEAP1 superbinder mutants enhances nuclear localization of NRF2
 A, H2228 cells were co-transfected with the indicated FLAG-tagged *KEAP1* mutant plasmid or negative control Venus-*NPM1*, and *NRF2* plasmid. Cells were lysed in RIPA buffer and analyzed by Western blot for the indicated proteins. B, A549 cells were transiently transfected with the indicated *KEAP1* mutants or Venus-*NPM1*, and protein lysates were analyzed as described in (A). C, HEK293T cells were transiently transfected with the indicated FLAG-tagged *KEAP1* mutants. Cells were fractionated into nuclear and cytoplasmic fractions and lysates were analyzed by Western blot for the indicated endogenous (*NRF2*, MEK1/2, H3) and ectopically expressed proteins.

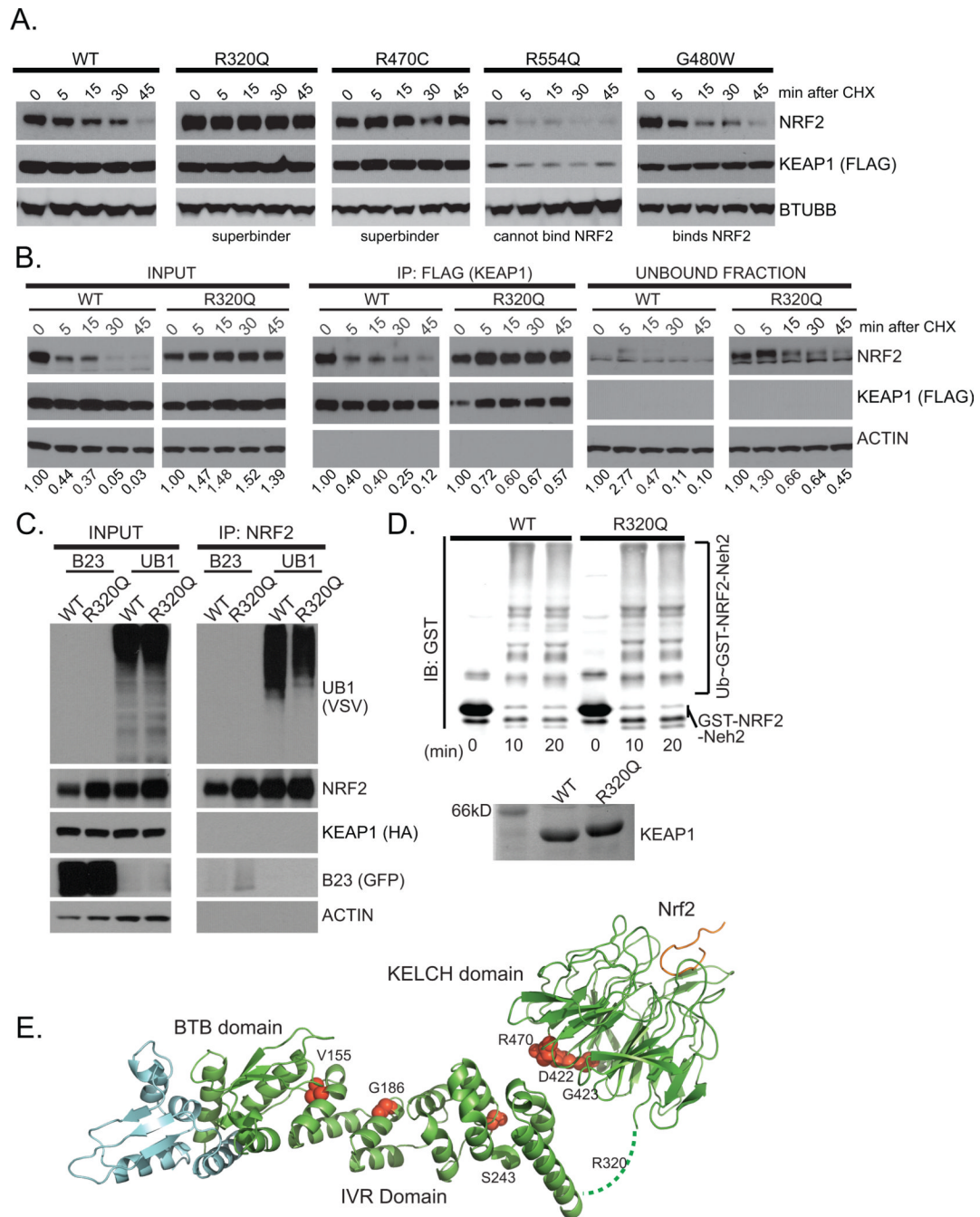


Figure 5. KEAP1 superbinder mutants cannot degrade NRF2 but maintain the ability to ubiquitinate NRF2

A, HEK293T cells stably expressing the indicated FLAG-tagged *KEAP1* mutants were transiently transfected with *NRF2*. Cells were treated with 50 $\mu\text{g}/\text{mL}$ cycloheximide (CHX) for the indicated time, and cell lysates were analyzed by Western blot for the specified proteins. B, HEK293T cells stably expressing the indicated FLAG-tagged *KEAP1* mutants were treated with CHX as described in (A). FLAG immunoprecipitation was performed to isolate protein complexes containing the indicated *KEAP1* mutants. Whole cell lysate (INPUT), immunoprecipitated complexes (IP:FLAG), and eluate (UNBOUND FRACTION) were analyzed by Western blot for the indicated proteins. Values represent NRF2

quantitation relative to FLAG-tagged KEAP1 expression. C, HEK293T cells stably expressing either FLAG-tagged wild-type KEAP1 or the R320Q mutant were transfected as described in (A). Cells were lysed under denaturing conditions, and then diluted to physiological pH in 0.1% NP-40 lysis buffer. Immunopurification of NRF2 was performed, and protein complexes were analyzed by Western blot. D, Purified KEAP1 or the R320Q mutant was mixed with recombinant human E1, UbcH5, CUL3-RBX1, ubiquitin and GST-tagged NRF2 NEH2 domain. Ubiquitinated NRF2 was detected by Western blot analysis. E, The BTB and IVR domains of KEAP1 (green) were modeled by the I-TASSER server. The BTB domain of the second copy of KEAP1 within the dimer is shown in cyan. Superbinder residues are shown in red spheres. R320 is located in a predicted short linker connecting the BTB-IVR domain and KELCH domain.